

Ultra Wide Band transmitter design for a vital sign monitoring passive tag

Julia Borges Silva
Faculdade do Gama
Universidade de Brasília
Brasília, Brazil
juliaborges.6@gmail.com

Wellington Avelino do Amaral
Faculdade do Gama
Universidade de Brasília
Brasília, Brazil
waamaral@unb.br

Ciro Barbosa Costa
Faculdade do Gama
Universidade de Brasília
Brasília, Brazil
ciro.barbosacosta@gmail.com

Abstract—The following work aims to develop a Ultra Wide Band (UWB) transmitter as a sub-block of an Radio Frequency Identification (RFID) tag for remote monitoring of vital signs such as heart rate, breath rate, and body temperature without human contact. This need is especially relevant in pandemic scenarios like the current one caused by the SARS-Cov-2 virus. The study includes topology analysis of the UWB transmitter, corners simulation, and layout with the aim of manufacturing a transmitter as a subsystem of a biomedical integrated circuit tag. The simulation results show that the energy per pulse was around 100 pJ, as expected, and pulse delay was controlled using a 1.2 V voltage source. The output had peak values between 200 and 600 mV, with a bandwidth between 3 and 10 GHz, suitable for communication with other devices of varying technologies. The power consumption of the transmitter was found to be similar to that of other medical-use transmitters. Due to area constraints, a part of the circuit had to be separated from the chip, and a printed circuit board was developed for future external integration. The results of this study indicate that the developed UWB transmitter can be helpful for remote monitoring of vital signs, and future work can focus on integrating the circuit onto the chip and testing the transmitter’s performance in combination with an antenna for transmission and range testing.

Index Terms—UWB, RFID, biomedical, layout

I. INTRODUCTION

Radio-frequency identification technology (RFID) is replacing barcodes due to its practicality in transmitting and receiving information. Moreover, RFID presents information in a non-visible manner on items. The fact that passive RFID technology makes low-cost tags available has significantly contributed to its extensive use in several applications, including barcode replacement, biomedical applications, and location applications. This, in turn, has led to increased technological demands [1].

To fulfill the requirements of greater operating range, higher data transmission rates, higher resolution for accurate location, and less sensitivity to interference, UWB technology is utilized in conjunction with the tag as a promising solution to address the limitations associated with low bandwidth, however, with issues related to powering a UWB receiver. A hybrid UHF/UWB technology is employed so that the UWB circuit

transmits data at high rates with lower sensitivity, while the Ultra High Frequency (UHF) enables tag control and power-up. During the uplink, the recovered energy from the UHF is utilized to power the IR-UWB (impulse ultra wideband radio) transmitter, which sends data for a brief period at high rates [2].

The SARS-CoV-2 virus pandemic caused a crisis in the healthcare systems of countries, as hospitals were overwhelmed with cases of the disease, which had no specific treatment, and lacked sufficient space and equipment for all necessary hospitalizations. Thus, the COVID-19 crisis has highlighted the need for remote monitoring of critical information such as respiratory rate, heart rate, and temperature of patients without the need for human contact, allowing for home care of less severe cases as well as other viral and even chronic diseases.

As depicted in Figure 1, the tag attached to the patient’s chest would continuously monitor vital signs, which can be transmitted via wireless communication to other devices, making the patient’s data readily available in the cloud in an efficient and convenient manner for both the patient and the hospital. Furthermore, as shown in Figure 1, the developed tag incorporates a receiver for vital signs and an energy-harvesting power supply.

Figure 2 delineates the block diagram of the biomedical tag and its operational process at a high level. Firstly, the

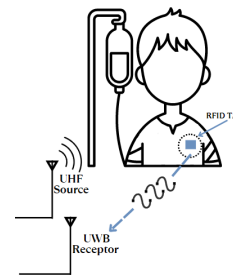


Fig. 1. Wearable tag for vital signs monitoring.

receiving antenna is linked to the rectifier, which is responsible for receiving UHF signals and converting them into a DC voltage level. The resultant voltage level is then utilized to power the other blocks of the polarization block, wherein the Low-dropout regulator (LDO) regulates the 1.8 V input voltage to a 1.2 V signal generated by the voltage reference block. Subsequently, the output of the LDO is used to power the temperature sensor, the modulation block, and the transmitter. These components collaborate to prepare the data for transmission through the UWB antenna. Lastly, the ADC (analog-to-digital converter) is an external circuit that is anticipated to be integrated into the remaining project's parts in future versions. This design is based on [8], which also designs and tests a wearable monitor tag, with a different polarization block, modulation, and transmitter size.

With the overall context above, the present work is dedicated to the design of a UWB transmitter that is in charge of the processing of digital data of the patient to be sent in CMOS 0.18 μm UMC technology. The system comprises of a pulse generator and filter with digital input and a 1.2 V DC analog power supply. The system expected output is a monocyclic Gaussian pulse format. The essential criteria for the transmitter's design are to control the duration and width of the pulse and ensure low power consumption in the pJ scale.

II. CIRCUIT DESIGN

The generation of UWB pulse typically involves three main topologies: LC oscillators, which utilize an inductor and capacitor with active load, architectures that combine a digital pulse generator with pulse formatting, and ring oscillators. While LC circuits are capable of achieving high efficiency, they also have high power consumption. In contrast, ring oscillators are activated for short periods of time, have low noise, and utilize digital logic, but have high static consumption and low switching speed [5].

Consequently, the selected architecture is the pulse generator with a pulse formatting stage, as it provides the advantage of using simple circuits that delay the pulse and generate a monocyclic Gaussian wave with low power consumption and high transmission rate [6]. Figure 3 depicts the sub-blocks of this topology, consisting of a pulse generator that receives the digital information from the modulation and generates a UWB pulse, and a pulse formatter block that shapes the monocyclic

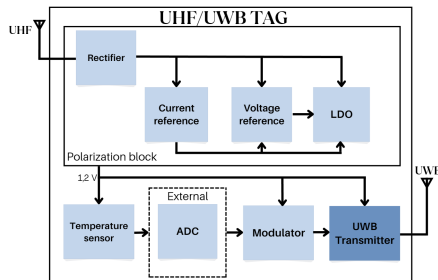


Fig. 2. Block diagram of the complete tag project for measuring vital signs

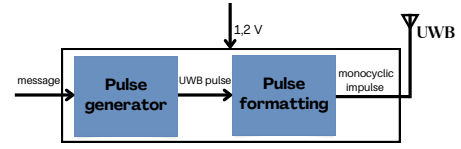


Fig. 3. High-level block diagram of the chosen transmitter.

pulse. The resultant RF signal will be transmitted by the tag antenna, while the polarization block provides the 1.2 V DC supply to the circuit.

The required components for the generator include inverters and delay cells that consist of an inverter with a capacitor at the output. These modules are interconnected in a manner that allows the input signal to be split into multiple delays, which are then used as inputs to a logic gate for generating the UWB pulse. The choice between a NOR or NAND topology for the logic gate is possible, with the main difference being that in the former, a positive impulse is generated by adjusting the time difference between two low-voltage signals, while in the latter, a negative impulse is generated when the inputs have a high voltage value [7]. As a positive sign is desired, the NAND gate is utilized.

Specifically for the transistors of the inverter, the width-to-length ratio is designed based on (1) [7]. μ is the magnetic permeability of the transistor $(\frac{W}{L})_n$ and $(\frac{W}{L})_p$ being the width-to-length ratio of the n-type and p-type transistors, respectively.

$$\frac{(\frac{W}{L})_n}{(\frac{W}{L})_p} = \frac{\mu_p}{\mu_n} \quad (1)$$

A. Delay cell

One of the desirable functions implemented in the present work is an adjustable pulse generator, capable of generating pulses with varying durations but the same format, in order to achieve different objectives. This approach results in a flexible circuit that enables the generation of pulses with longer durations, which contain more low-frequency components, and hence can propagate over longer distances with minimal losses. Conversely, pulses with shorter durations have higher bandwidth and greater resolution [7].

Figure 4 illustrates the basic structure of the circuit, with M1 being the controlled transistor and M2 the capacitor. V_{ctrl} is used to adjust the resistance of the transistor and, together with the capacitance M2, acts as the load of the output logic. By varying this control voltage, the equivalent capacitance at the inverter output can be adjusted. Specifically, a high voltage value reduces the resistance of the shunt transistor M1, increases the capacitance, and results in a longer delay [7].

To estimate the delay generated by the cascaded inverters, the load capacitance at the output of the N-th inverter has to be considered, C_{load} , as well as the input capacitance of the first inverter, C_{load} , the effective switching resistance of the first inverter $R_{n,p1}$ and a A factor defined by (2). The delay equation is presented in (3) [7].

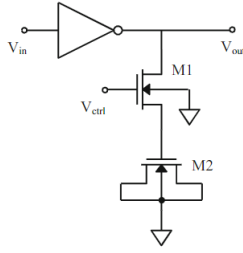


Fig. 4. Inverter and delay element Source.

$$A = \left(\frac{C_{load}}{C_{inN}} \right)^{1/N} \quad (2)$$

$$Delay = 0.7N(R_{n1} + R_{p1})(C_{out1} + A^N C_{in1}) \quad (3)$$

B. Pulse formatting

The passive filter shown in Figure 5 was selected based on the work of [8] and is a bandpass filter that combines a low-pass block and a high-pass block. The output of the logic gate is connected to the filter via an M0 driver transistor, which is included in the filter's capacitance. The NOR logic gate is employed in pulse formation, with an NMOS transistor being utilized that exits the cut-off region at positive voltages.

III. RESULTS

The effectiveness of the filter, its performance within the desired frequency band, and its impedance match were analyzed by evaluating the circuit's S parameters using Cadence's simulation environment. The results of this analysis, depicted in Figure 6, show that S21 has low loss within the 3 to 10 GHz frequency band, indicating that the filter functions as a bandpass filter. S22 represents the degree of match at the output and measures the level of reflection from the antenna. The results indicate that the filter is successfully reflecting the signal within the band of interest.

The power consumption of the circuit was simulated to be approximately 335 mW. The EPP (energy per pulse) was also calculated and found to be 100.5 pJ, which is consistent with the value reported by [8] for a similar biomedical tag using a UWB transmitter. It is noteworthy that the EPP is lower than that of circuits developed for WPAN applications, as studied by [9], where values of 224 pJ were reported. However, there is still potential for further reduction of EPP

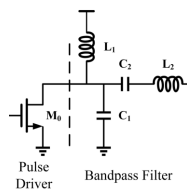


Fig. 5. Filter schematic [8].

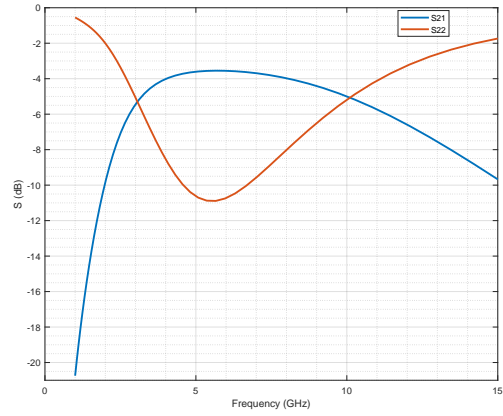


Fig. 6. Filter S-parameters

and circuit consumption peaks, as demonstrated in a study by [6], where a delay-based architecture with modifications in the pulse formatting stage, involving the addition of one more driver transistor and an LC filter in series, resulted in an EPP value of around 10 pJ.

A. Corners

Corner simulations were conducted for FF, SS, FS, and SF cases, incorporating variations in temperature and supply voltage. Furthermore, the control voltage was varied between the minimum (0 V) and maximum (1.2 V) to examine the behavior of the pulse in all cases and ensure its response is within expected. The worst output value, 108.19 mV peak, was observed with a control voltage of 1.44 V in the SS scenario and the best case was with a control voltage of 1.2 V in the FS scenario, with a supply voltage of 0.96 V and an output peak at 1 V. In all corners, the circuit exhibited the expected behavior, indicating its capability to transmit in different scenarios of power supply, temperature, voltage control, and component manufacturing extremes.

B. Layout

The layout of the UWB transmitter was developed for later integration with the tag layout. To ensure that it is consistent with the schematic, a round of simulations was performed on the model after the parasitic extraction phase, yielding satisfactory results for control voltages of 0 V and 1.2 V with a 1.2 V square wave as an input to simulate the digital signal received by the ADC and modulator blocks from 2. As shown in Figure 7, by varying the control voltage it is possible to see the difference in delay and peak value of the pulse. As expected, the higher the voltage, the higher the peak and the longer the pulse time, which has the expected form of a monocyclic Gaussian.

However, during the integration phase of the tag layouts to create the complete tape-out file, it was concluded that the filter circuit design would not fit. As a result, changes were made in the layout to ensure that the pulse generator circuit remained integrated, for connection with a PCB for the filter. This required redoing the layout with surface-mount

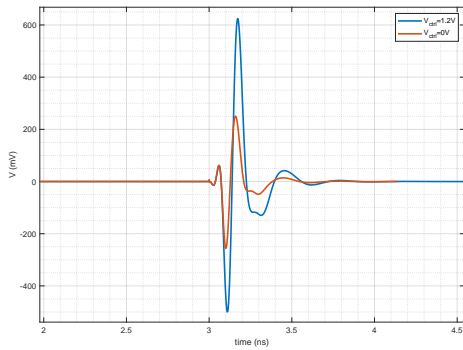


Fig. 7. Post layout simulation with multiple control voltages.

device (SMD) capacitors and inductors capable of operating within the UWB voltage and frequency range. Thus, the driver continued as part of the integrated circuit, functioning as an interface between the tag and the new board, generated using the free EasyEDA software. Figure 8 the tag layout, with the transmitter position highlighted in red.

For the final layout, which was integrated into the chip, a new simulation was generated after extracting the parasitic components, as shown in Figure 9. The thicker line represents the signal after passing through the transistor driver, and the thinner line shows the signal after leaving the pulse generator, with larger peaks due to the lack of filtering and noise distorting the beginning and end of the pulse. The blue signal, on the other hand, demonstrates the function of the driver transistor in formatting the wave, this being the signal that will feed the external filter and antenna on the Printed Circuit Board (PCB).

With that, the transmitter is ready for production and later bench testing.

IV. CONCLUSION

This paper presents the development of an ultra-wideband (UWB) transmitter, starting from the circuit topology and extending to the layout of a printed circuit board and parasite extraction. Due to space limitations, the pulse generator and

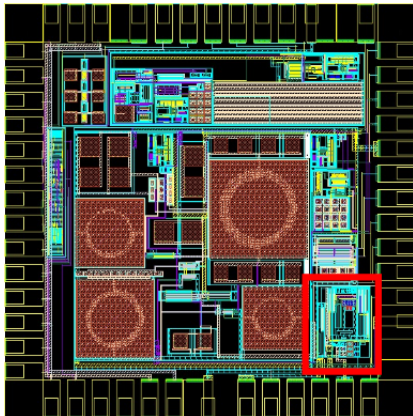


Fig. 8. Tag layout

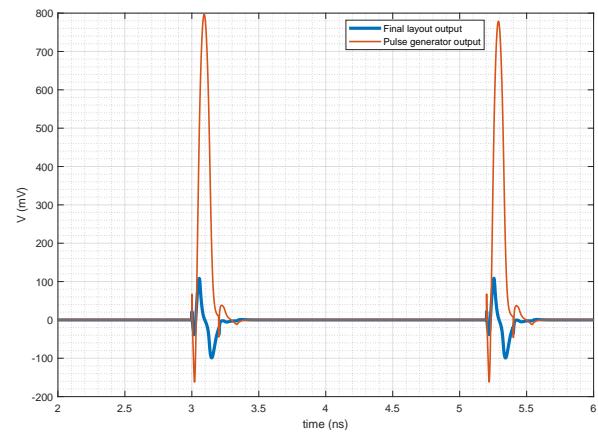


Fig. 9. Post layout final simulation

filter transistor had to be integrated with the capacitors and inductors. The results of the simulation showed an EPP of around 100 pJ, with peak values between 200 mV and 600 mV and a band between 3 and 10 GHz. The circuit fulfilled the objectives of low consumption, transmitter signal delay control, parasite extraction simulations, and layout elaboration.

For future improvements, it is suggested to insert a resistor in the filter between the low-pass and high-pass blocks to improve the match and the output pulse format. Additionally, it is possible to explore a topology without the bandpass filter to decrease the EPP but with costs in the bandwidth. Testing the circuit and integrating the tag into an antenna for additional transmission and range tests is also necessary when the produced chip arrives, later this year.

REFERENCES

- [1] DARDARI, D. et al. "The future of ultra-wideband localization in rfid". 6 IEEE International Conference on RFID, 2016.
- [2] ZOU Z., T. H.; LANDE, T. Impulse radio uwb for the internet-of-things a study on uhf/uwb hybrid solution. KTH School of Information and Communication Technology., 2012.
- [3] OPAS. "Folha informativa sobre COVID-19". 2022. Available on: <https://www.paho.org/pt/covid19>.
- [4] SAÚDE, M. da. "Sala de Situação de Monkeypox (Desativada)". 2022. Available on: <https://www.gov.br/saude/pt-br/composicao/svs/resposta-a-emergencias/sala-de-situacao-de-saude/sala-de-situacao-de-monkeypox>. Access on: 21 set. 2022.
- [5] FAHS, B.; ALI-AHMAD, W.; GAMAND, P. A two-stage ring oscillator in 0.13- μm cmos for uwb impulse radio. *Microwave Theory and Techniques*, IEEE Transactions on, v. 57, p. 1074 – 1082, 06 2009.
- [6] RAMAZANOGLU, S.; DUNDAR, G.; BATUR, O. Design and comparison of low power pulse combining ir-uwb transmitters in 180nm cmos. In: . [S.l.: s.n.], 2019. p. 97–100.
- [7] NGUYEN, C.; MIAO, M. "Design of cmos rfc ultra-wideband impulse transmitters and receivers."
- [8] LYU, H.; WANG, Z.; BABAKHANI, A. "A uhf/uwb hybrid rfid tag with a 51-m energy-harvesting sensitivity for remote vital-sign monitoring". *IEEE Transactions on Microwave Theory and Techniques*, v. 68, n. 11, p. 4886–4895, 2020.
- [9] DIAO, Y. Z. S.; HENG, C.-H. A cmos ultra low-power and highly efficient uwb-ir transmitter for wpan applications. *IEEE TCAS*, v. 56, p. 200–204, 2009.